



Structural and vascular changes in glaucoma with single-hemifield defect: predictors of opposite hemifield visual field progression

Anna Lee¹ · Kyung Rim Sung¹

Received: 31 May 2022 / Revised: 13 December 2022 / Accepted: 9 January 2023 / Published online: 20 January 2023
© The Author(s), under exclusive licence to Springer-Verlag GmbH Germany, part of Springer Nature 2023

Abstract

Purpose To investigate longitudinal changes in optic nerve head (ONH) superficial vessel density (VD), macular VD, circumferential retinal nerve fiber layer (RNFL) thickness, and macular ganglion cell-inner plexiform layer (GCIPL) thickness, and their associations with future VF defects in unaffected hemifields of primary open angle glaucoma (POAG) eyes with baseline VF defect confined to a single hemifield.

Methods This retrospective observational study included 61 POAG eyes with VF defect confined to a single hemifield monitored over a mean follow-up time of 2.7 years. Development of VF defect in opposite hemifield was defined based the Early Manifest Glaucoma Trail criteria. Each eye was classified into either “conversion” or “no conversion” groups according to development of VF defect in the unaffected hemifield. The rates of longitudinal changes in VD and structure parameters in each hemiretina were compared between the two groups. A Cox proportional hazard model was used to identify potential risk factors for VF conversion in the unaffected hemifield.

Results Among 61 eyes, 17 eyes (27.9%) were classified as “conversion” and 44 eyes (72.1%) were classified as “non-conversion” groups. The conversion group exhibited significantly greater rates of both VD and structural changes in both hemiretinas. In Cox proportional hazard model, greater rate of change in GCIPL thickness, ONH superficial VD, and macular VD of both hemiretinas and greater rate of change in RNFL thickness of the unaffected hemiretina were identified as risk factors for VF conversion in the unaffected hemifield.

Conclusions Monitoring progressive changes in VD and structural parameters effectively predict future VF defect in the opposite hemifields of POAG eyes with single-hemifield defects.

Key messages

- Progressive vessel densities (VDs) and structural loss have been known to be associated with VF progression.
- Serial measurements of VDs using optical coherence tomography (OCT) angiography and structural changes assessed by OCT are useful for prediction of future glaucomatous conversion in the perimetrically unaffected hemifields of glaucomatous eyes with single-hemifield defects.
- Monitoring of both perimetrically affected and unaffected hemiretina to detect worsening of pre-existing defects and development of new damage could be clinically useful in monitoring glaucomatous eyes with a single-hemifield defect.

✉ Kyung Rim Sung
sungeye@gmail.com

¹ Department of Ophthalmology, College of Medicine,
University of Ulsan, Asan Medical Center, 388-1
Pungnap-2-Dong, Songpa-Gu, Seoul, South Korea 138-736

Keywords Single-hemifield defect · Glaucoma · Progression · Optical coherence tomography angiography · Vessel density

Introduction

Glaucomatous visual field (VF) defect often begins with the horizontal meridian, consistent with the classic retinal nerve fiber layer (RNFL) raphe pattern [1]. The progression pattern of VF defect is generally consistent with retinal nerve fiber bundle orientation, thereby leading to spread within a single (superior or inferior) hemifield until advanced stages of glaucoma [1]. Because VF defect in both hemifields could threaten patients' vision and fixations, expansion of VF defect to the opposite unaffected hemifield in eyes with single-hemifield defect at baseline could be a warning sign for disease progression, necessitating more aggressive treatments in these cases.

Measurement of RNFL thickness using optical coherence tomography (OCT) is known to be useful for detection of glaucoma, as structural changes are frequently detected prior to manifestation of overt VF defects [2]. Furthermore, initial RNFL thinning, as well as more rapid RNFL thinning, are known risk factors for future VF defects [3–6]. Thus, serial measurements of RNFL thickness are widely used to monitor progression of glaucoma. This is used concurrently with serial OCT and OCT angiography (OCT-A) measurement of vessel density (VD) in the peripapillary area and macula, which in the case of OCT-A only recently became widely available in clinical practice [7, 8]. Prior studies reported that development of VD loss and more rapid progression of VD loss are independently associated with VF progression [9–11]. Therefore, OCT-A measurement of VD could be a useful biomarker to predict VF progression, in addition to standard structural parameters measured by OCT.

Previous case–control studies have reported that the perimetrically unaffected hemiretinas of primary open-angle glaucoma (POAG) eyes with single-hemifield defect exhibit significantly reduced RNFL thicknesses and VD compared with normal eyes [12–14]. Nonetheless, little is known regarding the potential association between structural and/or vascular deterioration and future VF defects in unaffected hemifields. Because more rapid structural and vascular decline is associated with faster VF progression, we hypothesized that the rates of changes to structural and vascular parameters could be associated with development of VF defect in the unaffected hemifield of glaucomatous eyes with current single-hemifield defect. Hence, in the present study, we sought to investigate progressive changes of structural and vascular parameters in POAG eyes with single-hemifield VF defect and identify factors associated with future development of VF defect in the perimetrically unaffected hemifield using OCT and OCT-A.

Methods

Study subjects

This retrospective observational study was approved by the Institutional Review Board (IRB) of Asan Medical Center, and all procedures were conducted in accordance with the tenets of the Declaration of Helsinki. The requirement for informed consent from study subjects was waived by the Asan Medical Center IRB due to the retrospective study design.

Medical records of patients that visited our glaucoma clinic at Asan Medical Center from November 2016 to December 2021 were consecutively reviewed. All included patients underwent an initial comprehensive ophthalmic work-up including a medical history review, measurement of best-corrected visual acuity (BCVA), measurement of intraocular pressure (IOP) using Goldmann applanation tonometry, slit-lamp biomicroscopy, refractive error analyses using an autorefractor (KR-890; Topcon, Tokyo, Japan), axial length measurement (IOL Master version 5; Carl Zeiss Meditec, Dublin, CA, USA), central corneal thickness (CCT) measurement using ultrasound pachymetry (Tomey SP-3000, Nagoya, Japan), dilated color fundus photography (Canon, Tokyo, Japan), optic disc stereoscopic photography, red-free RNFL photography (Canon), Humphrey field analyzer Swedish Interactive Threshold Algorithm -Standard 24–2 VF testing (Carl Zeiss Meditec), spectral-domain optical coherence tomography (SD-OCT; Cirrus HD; Carl Zeiss Meditec), and imaging with a commercial OCT-A system (Angiovue; Optovue, Inc., Fremont, CA, USA).

The present study enrolled POAG cases that met the following pre-determined inclusion criteria: (1) age \geq 18 years; (2) BCVA \geq 20/30; (3) spherical equivalent between -6.0 and $+3.0$ diopters (D) and a cylinder correction within ± 3 D; (4) normal anterior and posterior chamber with open angles on slit lamp exam and gonioscopy; (5) at least five serial VF tests, excluding the first VF test, with a mean deviation (MD) better than -20.00 dB at baseline and at least four serial SD-OCT and OCT-A scans every 6–12 months during a minimum 2-year follow-up period; to account for the learning effect in VF tests, a second VF test was conducted within 1 week if the first VF result indicated glaucomatous damage; (6) the presence of a glaucomatous optic disc change (i.e., focal or generalized neural rim loss and localized or diffuse RNFL atrophy) with compatible glaucomatous VF defects [15]; and (6) glaucomatous VF defects confined to a single hemifield. Eyes with glaucomatous VF defects confined to a single-hemifield were defined by (1) a

cluster of ≥ 3 points on a pattern deviation probability map with $P < 0.05$, or with ≥ 2 points with $P < 0.02$ on a pattern deviation probability map in a single-hemifield (superior or inferior); (2) no clusters of three points with $P < 0.05$ or two points with a P -value < 0.02 on both the total deviation and pattern deviation probability maps in the opposite hemifield; and (3) a glaucomatous hemifield test result outside normal limits, which was confirmed on 2 consecutive reliable VF tests [16].

Subjects with one or more of the following conditions were excluded: (1) history of intraocular surgery, trauma, or laser treatment during follow-up; (2) severe media opacities such as dense cataract or vitreous opacity, which compromise SD-OCT/OCT-A scan quality and validity of VF test results; (3) ocular/systemic diseases or severe myopic ONH/macular changes, which could impair adequate ONH/VF/SD-OCT/OCT-A evaluation; and (4) unreliable VF results or poor-quality SD-OCT/OCT-A scans.

SD-OCT imaging

RNFL thickness and macular ganglion cell-inner plexiform layer (GCIPL) thickness were measured using Cirrus high-definition (HD) SD-OCT software (version 10.0). RNFL data were obtained using an optic disc cube in 200×200 scan mode, which scans a 6×6 mm square centered on the

ONH. The average RNFL thickness was measured in a 3.2-mm circle. The Cirrus HD SD-OCT software automatically provides RNFL thickness values globally and for each sector of four quadrants. The superior and inferior the RNFL thickness were used to represent the RNFL thickness of two hemiretinal regions; for example, the perimetrically affected and unaffected hemiretina (Fig. 1b).

For assessment of macular structural change, we measured GCIPL thickness because Cirrus HD SD-OCT automatically provides GCIPL thickness for macular structural parameter. GCIPL thickness was measured in the macular region, centered on the fovea. GCIPL thickness was measured within an annulus with inner vertical and horizontal diameters of 1 and 1.2 mm, and outer vertical and horizontal diameters of 4 and 4.8 mm, respectively. Superior GCIPL thickness was estimated for the superior hemiretina by averaging superior temporal, superior center, and superior nasal measurements. Accordingly, inferior hemiretina GCIPL thickness were estimated by averaging measurements of the inferior nasal, inferior center, and inferior temporal sectors (Fig. 1c).

Only images with a signal strength > 7 were included in analysis. SD-OCT images were excluded if one or more of the following defects was present: (1) motion artifacts, (2) poor centering on the fovea, or (3) segmentation errors.

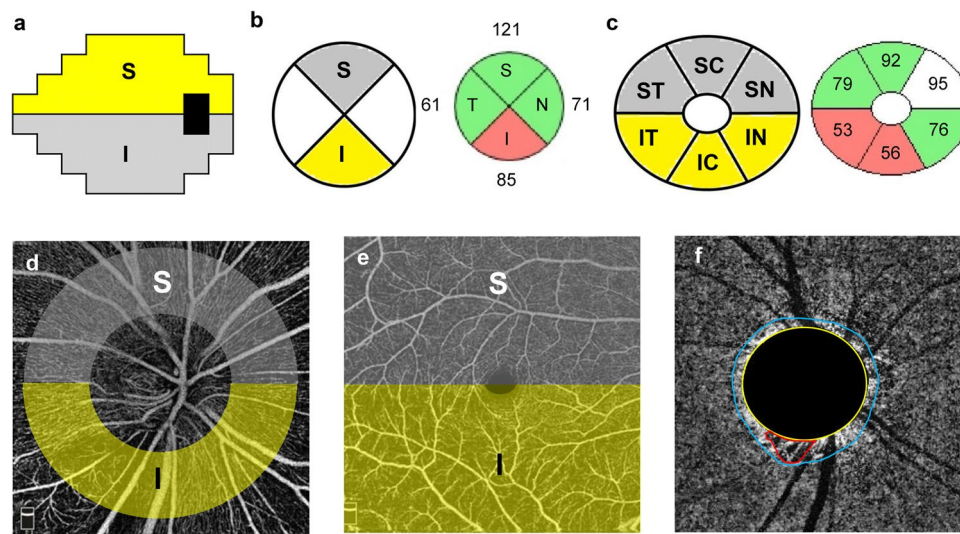


Fig. 1 Determination of the perimetrically affected and unaffected hemifields. Schematic illustration of the **a** visual field, **b** retinal nerve fiber layer thickness map, **c** macular ganglion cell-inner plexiform layer thickness map, **d** optic nerve head (ONH) superficial vessel density map, and **e** macular vessel density map. The yellow and gray colors represent perimetrically affected and unaffected hemifields, respectively. **f** En face choroidal layer vessel density maps represent the presence of choroidal microvasculature dropout (CMvD) within β

-zone parapapillary atrophy (β -PPA) which is demarcated by red outline. Yellow and blue outlines indicate the margin of the ONH and β -PPA, respectively. β -PPA, β -zone parapapillary atrophy; CMvD, choroidal microvasculature dropout; I, inferior; IC, inferior center; IN, inferior nasal; IT, inferior temporal; N, nasal; ONH, optic nerve head; S, superior; SC, superior center; SN, superior nasal; ST, superior temporal; T, temporal

OCT-A imaging

OCT-A imaging of the ONH and macular regions was performed using an AngioVue OCT-A system (Optovue Inc). ONH superficial VD measurements were taken using images of $4.5 \times 4.5 \text{ mm}^2$ scans centered on the optic disc within the radial peripapillary capillary slab from the internal limiting membrane to the nerve fiber layer after automated removal of large retinal vessels. Macular VD measurements were calculated from whole en face image VD derived from the entire $6 \times 6 \text{ mm}^2$ region centered on the fovea within slabs ranging from the internal limiting membrane to the posterior boundary of the inner plexiform layer. The OCT-A software automatically provided peripapillary and macular region VD, which were divided into the superior and inferior hemiretina (Fig. 1d, e).

Assessment of choroidal microvasculature dropout (CMvD) within β -parapapillary atrophy (β -PPA) was evaluated on en face images derived from $4.5 \times 4.5 \text{ mm}$ choroidal layer vessel density maps generated by ONH OCT-A (Fig. 1f) [17]. These slabs contained layers from the retinal pigment epithelium to $390 \mu\text{m}$ below the Bruch's membrane, which includes the full thickness of the choroid and the inner scleral border [18]. The presence of CMvD was defined according to the method described by Suh et al. [17]. Briefly, CMvD within the β -PPA was defined as a complete loss of the choriocapillaris or the microvasculature on en face choroidal layer vessel density maps [17, 19–21]. β -PPA was defined as an area between the optic disc margin as the inner margin of the peripapillary scleral ring on the scanning laser ophthalmoscopy images of OCT-A [22]. Dropout was required minimum width of $200 \mu\text{m}$ based on the approximated width of the central retinal vein in glaucomatous eyes via a previously validated method [23]. All en face choroidal layer images were evaluated independently by two glaucoma specialists (A.L. and K.R.S.), who identified the margins of the optic disc, β -PPA, and CMvD.

OCT-A images were excluded if one or more of the following defects was present: (1) poor image quality with signal strength index < 7 ; (2) motion artifacts such as significant residual motion line; (3) localized weak signal intensity caused by vitreous floaters or poor clarity such as that caused by media opacity; (4) images not centered on the fovea (fixation error); or (5) segmentation failure.

Development of visual field defect in unaffected hemifields

Development of VF defect in perimetrically unaffected hemifield was defined when three consecutive VF tests showed ≥ 3 points with $P < 0.05$ or ≥ 2 points with $P < 0.02$ on a pattern deviation probability map in an initial unaffected hemifield [24]. Patients with VF loss detected in

perimetrically unaffected hemifields during the follow-up period were classified into the “conversion” group. Conversely, patients without VF loss in perimetrically unaffected hemifields during the follow-up period were classified into the “no conversion” group.

Outpatient follow-up

After the initial comprehensive work-up, POAG eyes were managed with (97.4%) or without (2.6%) topical antiglaucoma medications based on patients' age, risk factors for disease progression, disease severity, level of IOP, and confirmation of disease progression. At the last follow-up, topical antiglaucoma medications were applied including prostaglandin analogues (83.4% of the patients), a combination of beta-blockers and carbonic anhydrase inhibitors (56.2%), and brimonidine (21.4%). Acceptable patient compliance with glaucoma medication was shown based on patient-reported adherence to antiglaucoma medication (taking $> 80\%$ of prescribed dose). The mean and peak follow-up IOP of the patients was $13.61 \pm 1.96 \text{ mmHg}$ and $15.42 \pm 2.47 \text{ mmHg}$, respectively.

Study endpoint definition

The endpoint for this study was evidence of VF progression defined as development of glaucomatous VF defect in three or more consecutive tests. For subjects with conversion, the study endpoint was defined as the first of three abnormal VF test dates. Conversely, subjects with no conversion did not reach the study endpoint.

Statistical analysis

All statistical analyses were performed using SPSS version 21.0 (IBM Corp, Chicago, IL). P -values < 0.05 were considered statistically significant, and results are presented as either mean values with standard deviation or as frequencies and percentages. The extent of interobserver agreement (A.L. and K.R.S) for the presence of CMvD was evaluated by the calculation of kappa (κ) coefficients. The normality of distribution was assessed using a Kolmogorov–Smirnov test. Normally distributed data were compared using an independent Student's t -test; otherwise, Mann–Whitney U tests were used. Categorical variables were compared using chi-square tests between groups. The total rate of change during a follow-up period on average in each eye was determined by linear regression analysis against patient age using serial OCT and OCT-A measurements. The change rates of each parameter were compared between the “conversion” and “no conversion” groups. Univariable and multivariable Cox proportional hazard models were performed to determine the risk factors for developing VF defects in perimetrically

unaffected hemifields. Variables with $P < 0.20$ in univariable analyses were included in multivariable analyses. For the final multivariable analysis, a backward elimination process was used.

Results

After an initial review, 77 eyes of 77 patients that met the initial inclusion criteria were included. Of these, six eyes with unreliable VF tests and ten eyes with poor OCT/OCT-A scan quality were excluded. A total of 61 eyes were included in the final cohort. Mean follow-up duration was 2.7 years and mean visit number was 5.1 visits. We found excellent interobserver agreements in CMvD measurement with $\kappa = 0.907$.

Table 1 summarizes baseline clinical characteristics of the participants. Among the 61 eyes, 17 eyes (27.9%) developed

glaucomatous VF conversion in the unaffected hemifield (conversion group) and 44 eyes (72.1%) did not (no conversion group). The conversion group exhibited significantly higher prevalence of CMvD (no conversion group = 52.3% vs. conversion group = 82.3%, $P = 0.031$) and lower baseline GCIPL thickness (average 76.0 vs. 69.9 μm ; affected hemifield 67.6 vs. 62.4 μm ; unaffected hemifield 85.4 vs. 78.2 μm , all $P < 0.05$). Average/regional RNFL thickness, ONH superficial VD, and macular VD values were generally lower in the conversion group, but the differences did not reach the statistical significance ($P > 0.05$).

Table 2 summarizes the total rates of change in OCT/OCT-A parameters over the following period on average between the two groups. Both affected and unaffected hemifields, the conversion group showed significantly greater rates of change in structural (RNFL thickness at affected hemiretina -0.06 vs. -1.31 $\mu\text{m}/\text{year}$; RNFL thickness at unaffected hemiretina -0.01 vs. -2.86 $\mu\text{m}/\text{year}$;

Table 1 Comparison of demographics and baseline clinical characteristics between eyes with and without glaucomatous visual field conversion in perimetrically unaffected hemifields

	All subjects	No conversion	Conversion	<i>P</i> -value
Number of eyes (%)	61 (100)	44 (72.1)	17 (27.9)	
Age, year	50.5 ± 13.5	49.9 ± 12.7	52.2 ± 16.0	0.597
Sex, male:female	36:25	29:15	7:10	0.078
Follow-up duration, year	2.7 ± 0.8	2.6 ± 0.8	3.0 ± 0.8	0.060
Axial length, mm	25.48 ± 1.78	25.56 ± 1.59	25.29 ± 2.20	0.654
Central corneal thickness, μm	527.05 ± 41.78	529.38 ± 42.03	520.94 ± 41.82	0.498
Intraocular pressure, mmHg	14.8 ± 3.1	14.9 ± 2.9	14.3 ± 3.9	0.581
Number of topical antiglaucoma medications, <i>n</i>	1.5 ± 1.0	1.5 ± 1.1	1.5 ± 0.7	0.962
CMvD, <i>n</i> (%)	37 (60.6)	23 (52.3)	14 (82.3)	0.031
Affected hemifield, S:I	53:8	38:6	15:2	0.786
Visual field mean deviation, dB	-7.11 ± 4.51	-6.91 ± 4.64	-7.62 ± 4.25	0.575
Global				
RNFL thickness, μm	70.6 ± 12.1	71.5 ± 10.4	68.1 ± 16.0	0.424
GCIPL thickness, μm	74.3 ± 9.6	76.0 ± 9.7	69.9 ± 8.0	0.018
ONH superficial VD,%	42.5 ± 4.9	43.2 ± 4.4	40.8 ± 5.7	0.129
Macular VD,%	41.7 ± 4.6	42.2 ± 4.4	40.3 ± 4.9	0.185
Perimetrically affected hemifields				
RNFL thickness, μm	63.5 ± 17.6	62.9 ± 13.7	65.0 ± 25.6	0.744
GCIPL thickness, μm	66.1 ± 9.1	67.6 ± 9.5	62.4 ± 7.3	0.031
ONH superficial VD, %	38.3 ± 5.0	38.6 ± 4.7	37.2 ± 5.6	0.380
Macular VD,%	39.0 ± 4.9	39.2 ± 4.3	38.4 ± 6.3	0.640
Perimetrically unaffected hemifields				
RNFL thickness, μm	101.5 ± 24.8	103.8 ± 24.8	95.6 ± 24.5	0.255
GCIPL thickness, μm	83.4 ± 11.1	85.4 ± 10.9	78.2 ± 10.1	0.021
ONH superficial VD, %	46.1 ± 6.0	46.9 ± 5.7	44.0 ± 6.4	0.117
Macular VD, %	44.1 ± 4.9	44.5 ± 4.9	42.9 ± 5.0	0.259

Boldface values indicate statistical significance

Continuous variables were compared by independent Student's *t*-test or Mann–Whitney *U* test

Categorical variables were compared by chi-square test

CMvD, choroidal microvasculature dropout; GCIPL, ganglion cell-inner plexiform layer; I, inferior; ONH, optic nerve head; RNFL, retinal nerve fiber layers; S, superior; VD, vessel density

Table 2 Comparisons of rates of change in OCT/OCT-A parameters between eyes with and without glaucomatous conversion in each hemifield

	Affected hemifield			Unaffected hemifield		
	No conversion	conversion	<i>P</i> -value	No conversion	Conversion	<i>P</i> -value
Rate of change in RNFL thickness, $\mu\text{m}/\text{year}$	-0.06 ± 2.03	-1.31 ± 1.34	0.008	-0.01 ± 4.19	-2.8 ± 2.79	< 0.001
Rate of change in GCIPL thickness, $\mu\text{m}/\text{year}$	-0.56 ± 1.49	-2.29 ± 1.73	0.002	-0.55 ± 1.12	-3.82 ± 3.04	< 0.001
Rate of change in ONH superficial VD, $\%/ \text{year}$	-0.64 ± 1.06	-1.66 ± 1.23	0.006	-0.55 ± 1.19	-1.48 ± 1.42	0.024
Rate of change in macular VD, $\%/ \text{year}$	-0.54 ± 1.60	-1.57 ± 1.46	0.022	-0.68 ± 2.01	-1.61 ± 1.06	0.023

Boldface values indicate statistical significance. Each *P*-value was estimated by Student's *t*-test

GCIPL ganglion cell-inner plexiform layer, *OCT* optical coherence tomography, *OCT-A* optical coherence tomography angiography, *ONH* optic nerve head, *RNFL* retinal nerve fiber layer, *VD* vessel density

GCIPL thickness at affected hemiretina -0.56 vs. $-2.29 \mu\text{m}/\text{year}$; GCIPL thickness at unaffected hemiretina -0.55 vs. $-3.85 \mu\text{m}/\text{year}$ and vascular parameters (ONH superficial VD at affected hemiretina -0.64 vs. $-1.66\%/ \text{year}$; ONH superficial VD at unaffected hemiretina -0.55 vs. $-1.48\%/ \text{year}$; macular VD at affected hemiretina -0.54 vs. $-1.57\%/ \text{year}$; macular VD at unaffected hemiretina -0.68 vs. $-1.61 \mu\text{m}/\text{year}$, all $P < 0.05$) compared to the no conversion group in both the affected and unaffected hemiretinas for all parameters.

Table 3 summarizes the Cox proportional hazard model for risk factors of development of VF defects in unaffected hemifields. To avoid multicollinearity between OCT and OCT-A parameters, two multivariable models were performed separately. Within the affected hemiretina, thinner baseline GCIPL thickness values (hazard ratio [HR], 1.090; 95% confidence interval [CI], 1.023 to 1.161; $P = 0.007$), a greater rate change in GCIPL thickness (HR, 1.283; 95% CI, 1.027 to 1.603; $P = 0.028$), a greater rate of change in ONH superficial VD (HR, 1.636; 95% CI, 1.074 to 2.494; $P = 0.022$), and a greater rate of change in macular VD (HR, 2.059; 95% CI, 1.354 to 3.131; $P = 0.001$) were significantly associated with the risk of developing VF defects in the perimetrically unaffected hemifield. Within the unaffected hemiretina, a greater rate of change in RNFL thickness (HR, 1.367; 95% CI, 1.130 to 1.655; $P = 0.001$), a greater rate of change in GCIPL thickness (HR, 1.432; 95% CI, 1.184 to 1.732; $P < 0.001$), a greater rate of change in ONH superficial VD (HR, 1.455; 95% CI, 1.001 to 2.115; $P = 0.049$), and a greater rate of change in macular VD (HR, 1.495; 95% CI, 1.123 to 1.990; $P = 0.006$) were associated with the future glaucomatous VF conversion in the perimetrically unaffected hemifield.

Figure 2 shows a representative case demonstrating progressive OCT/OCT-A parameter loss in a POAG eye with VF progression detected in the initial perimetrically unaffected hemifield during the follow-up. A 46-year-old woman with VF defect confined to the superior hemifield at baseline experienced expansion of VF defect across the horizontal meridian over a 3.8-year follow-up. Rates of ONH superficial

VD and macular VD changes exhibited progressive decrement in both the perimetrically affected (inferior ONH superficial VD $-0.96\%/ \text{year}$, inferior macular VD $-0.81\%/ \text{year}$) and unaffected hemiretinas (superior ONH superficial VD $-1.23\%/ \text{year}$, superior macular VD $-0.77\%/ \text{year}$). Additionally, GCIPL thickness also decreased in both the perimetrically affected (inferior GCIPL thickness $-0.90 \mu\text{m}/\text{year}$) and unaffected hemiretina (superior GCIPL thickness $-0.67 \mu\text{m}/\text{year}$) during the follow-up period. With regard to RNFL thickness, RNFL thickness of unaffected hemiretina showed progressive decrement over time (superior RNFL thickness $-0.88 \mu\text{m}/\text{year}$), but RNFL thickness of affected hemiretina did not show apparent change due to a floor effect (inferior RNFL thickness $-0.12 \mu\text{m}/\text{year}$).

Discussion

In the present study, the POAG eyes that developed a VF defect in the perimetrically unaffected hemifield exhibited significantly greater rates of change in OCT/OCT-A parameters in both the affected and unaffected hemiretina. Furthermore, greater structural and VD changes were significantly associated with future VF conversion in perimetrically unaffected hemifields. Our findings suggest that longitudinal assessment of vascular and structural changes is useful for clinical management of POAG eyes with single-hemifield VF defects and could predict risk of future VF conversion in perimetrically unaffected hemifields. In addition, progressive structure and vasculature deterioration could warrant more aggressive treatment to decrease the risk of VF conversion in the perimetrically unaffected hemifield.

Previous studies reported that eyes with glaucomatous progression showed more severe RNFL and GCIPL damage at baseline compared with those without [25, 26]. Lalezary et al. [25] reported that eyes with glaucomatous progression showed significantly thinner baseline RNFL thickness than those without. Zhang et al. [27] reported the utility of baseline focal macular thinning in predicting VF progression. The present findings are consistent with those of prior

Table 3 Univariate and multivariate Cox proportional hazard models for risk of future visual field damage in the perimetrically unaffected hemiretina

	Univariable model		Multivariable model 1 with OCT parameters		Multivariable model 2 with OCT-A parameters	
	HR (95% CI)	P-value	HR (95% CI)	P-value	HR (95% CI)	P-value
Affected hemiretina						
Age, 1 year older	1.012 (0.976–1.050)	0.542				
Refractive error, 1 diopter higher	1.040 (0.859–1.259)	0.691				
Axial length, 1 mm longer	0.987 (0.739–1.319)	0.926				
Central corneal thickness, 1 µm thinner	1.003 (0.991–1.014)	0.640				
Follow-up period, 1 year longer	1.253 (0.642–2.445)	0.509				
The presence of CMvD	3.091 (1.101–13.410)	0.035				
Baseline IOP, 1 mmHg higher	0.937 (0.788–1.114)	0.462				
Baseline VF MD, 1 dB worse	1.012 (0.916–1.119)	0.813				
Baseline RNFL thickness, 1 µm thinner	1.027 (0.986–1.070)	0.203				
Baseline GC IPL thickness, 1 µm thinner	1.060 (1.006–1.116)	0.029	1.090 (1.023–1.161)	0.007		
Rate of change in RNFL thickness, 1 µm/year faster	1.316 (1.024–1.690)	0.032	1.480 (0.982–2.232)	0.061		
Rate of change in GC IPL thickness, 1 µm/year faster	1.427 (1.182–1.722)	<0.001	1.283 (1.027–1.603)	0.028		
Baseline ONH superficial VD, 1 %lower	1.102 (0.998–1.216)	0.055				
Baseline macular VD, 1 % lower	1.103 (0.992–1.226)	0.071				
Rate of change in ONH superficial VD, 1 %/year faster	2.106 (1.397–3.174)	<0.001			1.636 (1.074–2.494)	0.022
Rate of change in macular VD, 1 %/year faster	1.756 (1.258–2.451)	0.001			2.059 (1.354–3.313)	0.001
Unaffected hemiretina						
Age, 1 year older	1.012 (0.976–1.050)	0.542				
Refractive error, 1 diopter higher	1.040 (0.859–1.259)	0.691				
Axial length, 1 mm longer	0.987 (0.739–1.319)	0.926				
Central corneal thickness, 1 µm thinner	1.003 (0.991–1.014)	0.640				
Follow-up period, 1 year longer	1.253 (0.642–2.445)	0.509				
The presence of CMvD	3.091 (1.101–13.410)	0.035	3.375 (0.872–13.054)	0.078	3.042 (0.855–10.827)	0.086
Baseline IOP, 1 mmHg higher	0.937 (0.788–1.114)	0.462				
Baseline VF MD, 1 dB worse	1.012 (0.916–1.119)	0.813				
Baseline RNFL thickness, 1 µm thinner	1.010 (0.992–1.028)	0.273				
Baseline GC IPL thickness, 1 µm thinner	1.055 (1.009–1.103)	0.018				
Rate of change in RNFL thickness, 1 µm/year faster	1.306 (1.097–1.556)	0.003	1.367 (1.130–1.655)	0.001		
Rate of change in GC IPL thickness, 1 µm/year faster	1.509 (1.273–1.790)	<0.001	1.432 (1.184–1.732)	<0.001		

Table 3 (Continued)

	Univariable model		Multivariable model 1 with OCT parameters		Multivariable model 2 with OCT-A parameters	
	HR (95% CI)	P-value	HR (95% CI)	P-value	HR (95% CI)	P-value
Baseline ONH superficial VD, 1 %/lower	1.065 (0.992–1.144)	0.080				
Baseline macular VD, 1 % lower	1.070 (0.970–1.180)	0.175				
Rate of change in ONH superficial VD, 1 %/year faster	1.672 (1.139–2.456)	0.009	1.455 (1.001–2.115)	0.049	1.455 (1.001–2.115)	0.049
Rate of change in macular VD, 1 %/year faster	1.468 (1.135–1.899)	0.003	1.495 (1.123–1.990)	0.006	1.495 (1.123–1.990)	0.006

Boldface values indicate statistical significance. Each P-value was estimated by Cox proportional hazard models

Multivariable model 1: CMvD, baseline GCIPL thickness, rate of change in RNFL thickness, the rate of change in GCIPL thickness

Multivariable model 2: CMvD, baseline macular VD, rate of change in ONH superficial VD, the rate of change in macular VD

CMvD, choroidal microvasculature dropout; CI, confidence interval; GCIPL, ganglion cell-inner plexiform layer; HR, hazard ratio; IOP, intraocular pressure; MD, mean deviation; OCT, optical coherence tomography; OCT-A, optical coherence tomography angiography; RNFL, retinal nerve fiber layer; VF, visual field; VD, vessel density

studies [25–28] in that conversion eyes exhibited significantly lower baseline GCIPL thickness in both affected and unaffected hemiretina than no conversion eyes (Table 1). These findings indicate that structural changes could already have been present in the macular region of the unaffected hemiretina before apparent VF conversion was detected. However, there was no significant difference in baseline RNFL thickness values in the affected hemiretina of both conversion and non-conversion groups. One possible explanation for these findings could be related to a “floor effect” of RNFL thickness in affected hemiretina. Although participants enrolled in the study had moderate severity of glaucoma with a mean MD of –7.10 dB, perimetrically affected hemifields were more severe than the mean VF MD. Because RNFL thickness is less sensitive than GCIPL thickness in advanced glaucoma [29–33], it is plausible that RNFL thickness of the affected hemiretina had already reached the measurement floor, and significant differences were not detectable between the two groups. There was no significant difference between the two groups in RNFL thickness at perimetrically unaffected hemiretina as well. One potential explanation is that loss of retinal ganglion cell counts in the macular region may be easier to detect than RNFL loss when evaluating early glaucomatous damage considering the high density of retinal ganglion cells in the macular region [34, 35]. A prior study [36] of 151 early-stage glaucoma eyes with a mean follow-up of 3 years demonstrated that GCIPL change was frequently detected prior to the corresponding RNFL change. Another explanation for the finding could be related to the study population, which consisted primarily of normal tension glaucoma cases (44 eyes, 72.1%). Because normal tension glaucoma is more closely associated with initial paracentral scotomas [37], VF conversion in the unaffected hemifield could begin in the paracentral area. Indeed, 70.6% of VF defects in the present study’s conversion group began within the paracentral area. Therefore, initial RNFL thickness in the unaffected hemiretina could be a poor predictor of glaucomatous conversion due to topographic disparities [38].

The rates of change in OCT/OCT-A parameters were significantly greater in the conversion group than in the no conversion group at both affected and unaffected hemiretina (Table 2). These findings suggest that eyes with glaucomatous progression spreading across the horizontal meridian exhibited significant progressive structural and vascular deterioration, not only in the apparently normal hemiretina, but also in the hemiretina corresponding to the pre-existing VF damage. Thereby, it is necessary to monitoring progressive structural and VD loss in the already-defective area as well as the intact area to detect potential glaucomatous progression in the unaffected hemiretina. Our findings are consistent with the findings of prior studies suggesting that glaucomatous progression occurs most frequently in areas with pre-existing abnormalities [39–42]. Boden et al. [41]

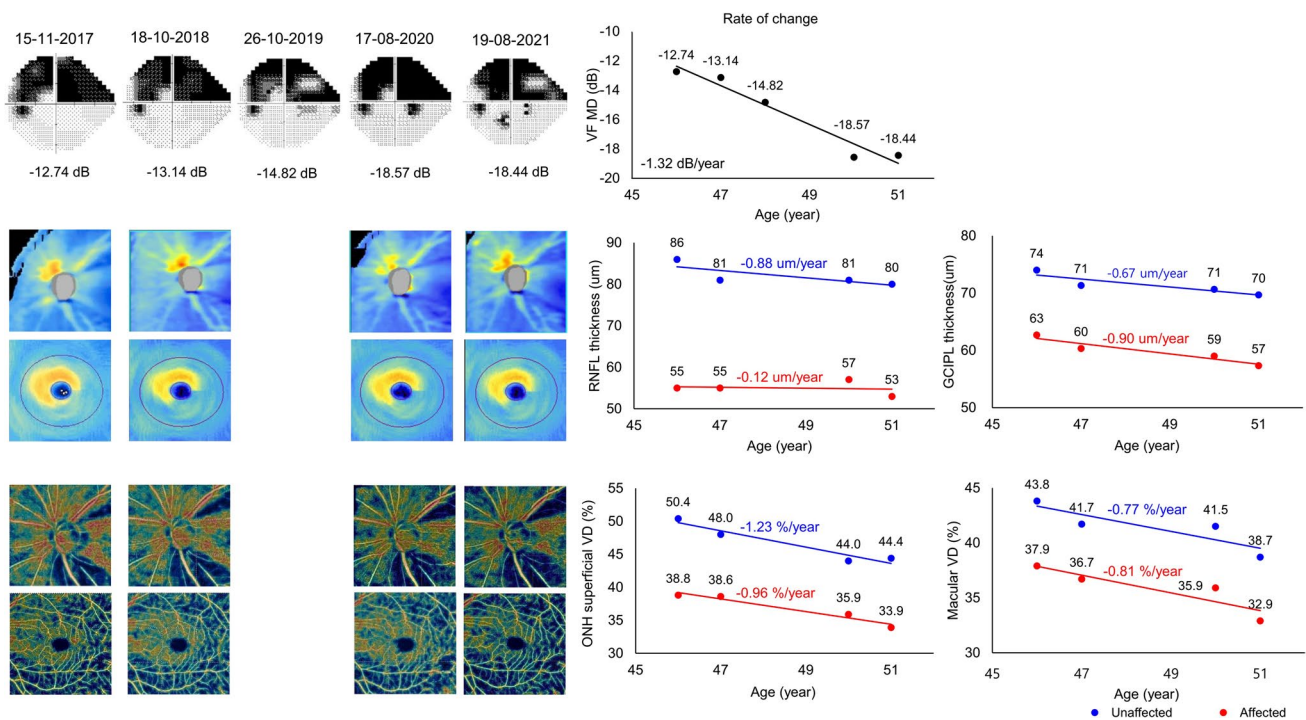


Fig. 2 A 46-year-old woman with visual field (VF) defect confined to the superior hemifield at baseline experienced expansion of VF defect across the horizontal meridian over a 3.8-year follow-up. Rates of optic nerve head (ONH) superficial vessel density (VD) and macular VD changes exhibited progressive decrement in both the perimetrically affected (inferior ONH superficial VD $-0.96\%/year$, inferior macular VD $-0.81\%/year$) and unaffected hemiretinas (superior ONH superficial VD $-1.23\%/year$, superior macular VD $-0.77\%/year$). Additionally, ganglion cell-inner plexiform layer (GCIPL) thickness also decreased in both the perimetrically affected (inferior

GCIPL thickness $-0.90 \mu\text{m}/year$) and unaffected hemiretina (superior GCIPL thickness $-0.67 \mu\text{m}/year$) during the follow-up period. RNFL thickness of unaffected hemiretina also showed progressive decrement over time (superior RNFL thickness $-0.88 \mu\text{m}/year$), but RNFL thickness of affected hemiretina did not show apparent change due to a floor effect (inferior RNFL thickness $-0.12 \mu\text{m}/year$). GCIPL thickness, macular ganglion-inner plexiform layer thickness; ONH, optic nerve head; RNFL, retinal nerve fiber layer; VD, vessel density; VF, visual field

reported that majority of progressed glaucoma eyes exhibited a combination of expansion and deepening of existing scotomas. Additionally, when the global MD rate of progression was compared with the progression rate of initial abnormal points, analyses suggested that most global progression is driven by the initially abnormal region [42].

In the Cox proportional hazard model (Table 3), greater rates of change in ONH superficial and macular VDs in both affected and unaffected hemiretina were the risk factors for future glaucomatous VF conversion of initial perimetrically unaffected hemifields. These results are consistent with recent findings that the rates of longitudinal changes in ONH superficial and macular VD are significantly associated with VF progression [10, 43]. Notably, the progressive VD changes in both affected and unaffected hemiretina were significantly associated with VF conversion. This supports our notion that VF conversion is associated not only with development of glaucomatous damage in an unaffected area, but also with worsening of pre-existing damage in an affected area. In our Cox proportional hazard model, the rates of change in GCIPL thickness in both affected and

unaffected hemiretina as well as the rate of in RNFL thickness in unaffected hemiretina were also the risk factors for VF conversion. These results are comparable to the previous studies that progressive structural loss had significantly higher risk for the glaucomatous progression [3, 44, 45]. However, the rate of change in RNFL thickness in affected hemiretina had no impact on VF conversion after controlling other covariates including the rate of change in GCIPL, despite having statistical significance in univariable analyses. One possible explanation for this finding is that RNFL exhibits a floor effect, below which no more change occurs. By contrast, GCIPL and VD have relatively larger dynamic range than RNFL [29, 46]. Thus, GCIPL and VD may be less susceptible to the floor effect even in affected hemiretina. That is why we think that the rates of change in GCIPL thickness and VD at affected hemiretina, not RNFL thickness, were better predictors of VF conversion.

There was no significant difference in baseline VD parameters between the conversion and no conversion groups (Table 1), and the baseline VD parameters of the perimetrically affected and unaffected hemiretina did not

affect subsequent development of VF damage in the perimetrically unaffected hemifield (Table 3). One possible explanation for this finding is that disruption of the superficial microvasculature could be secondary to axonal loss, such as RNFL thinning [17, 43], suggesting that significant differences in VD loss between the two groups were not detectable at baseline.

There are some inherent limitations in the study that should be considered. First, the findings should be cautiously interpreted due to the smaller sample size of the conversion group (17 eyes, 27.9%) than that of the no conversion group (44 eyes, 72.1%). Second, because the OCT-A device is newly adapted compared with the conventional OCT device, the study is limited by a relatively short follow-up period (2.7 years) and small number of OCT-A tests (5.1 tests). Third, RNFL thickness quadrants were used for analysis of perimetrically affected and unaffected hemiretina, which were topographically different each other, as explained in Fig. 1. Nevertheless, these regions are topographically close to each other, and no automatic reports for RNFL thickness hemiretina are currently provided by the Cirrus OCT device. Fourth, temporal region of RNFL was not considered in our study. RNFL thickness hemiretina may be insufficient to represent subtle change which begins within a localized region. Moreover, our cohort consisted of mainly NTG patients who may present paracentral scotoma. Because temporal region of ONH is topographically close to the macular vulnerability zone which was described by Hood et al. [47], temporal RNFL damage may be prior to hemiretinal RNFL change especially in patients with paracentral VF defect [47, 48]. Fifth, projection artifacts (i.e., overlying superficial retinal vessels) could make it difficult to precisely measure CMvD. Nonetheless, we excluded poor quality images from analysis to minimize any projection artifacts. In addition, two examiners independently evaluated CMvD with previously validated method [17, 19–21] and excellent interobserver agreements ($k=0.907$) were found. Sixth, we did not consider the potential confounding effects of ocular and systemic pressure-lowering medications on the rates of changes in OCT/OCT-A parameters. Alteration of ocular blood flow by systemic hypotensive medications could potentially affect OCT/OCT-A measurements. The use of topical IOP-lowering agents may also influence on OCT-A measured vessel densities. Martinez et al. [49] reported that intraocular blood flow increased after application of topical dorzolamide in both normal and glaucomatous eyes. Although topical combination IOP-lowering agents which including carbonic anhydrase inhibitor were applied 56.2% of our participants at the last follow-up, we did not consider the effect of carbonic anhydrase inhibitor on vessel density parameters. Seventh, as we evaluated a homogeneous Korean population that visited our tertiary clinic, our findings could potentially not be applicable to the general population. Moreover, inclusion

criteria regarding spherical equivalent (spherical equivalent -6.0 to $+3.0$ D; cylinder correction ± 3 D) and BCVA ($\geq 20/30$) could also limit the generalizability of our findings. Further large-scale studies with various ethnicities which can reflect real-world population will be necessary to exclude this possibility. Lastly, topographical disparities between the acquired horizontal axis of OCT/OCT-A images and the anatomic horizontal axis were not considered in the current study. He et al. [50] found that there were significant differences between acquired horizontal axis of SD-OCT images and the anatomic horizontal axis which connecting the fovea and Bruch's membrane opening. Therefore, these disparities may induce spurious functional loss in the wrong hemifield.

In conclusion, serial measurements of VD using OCT-A and structural changes assessed by OCT are useful for prediction of future glaucomatous conversion in the perimetrically unaffected hemifields of POAG eyes with single-hemifield defects. Progressive structural and vascular changes were detected in both perimetrically affected and unaffected hemiretina of eyes that presented VF conversion. Therefore, monitoring of both areas to detect worsening of pre-existing defects and development of new damage could be clinically useful in monitoring POAG eyes with a single-hemifield defect.

Author contribution Conception and design: K.R.S. Acquisition, analysis, and interpretation of data: A.L. and K.R.S. Drafting of the manuscript: A.L. and K.R.S. Statistical analysis: A.L. Supervision: K.R.S.

Availability of data and materials The datasets generated and/or analyzed during the current study are available from the corresponding author upon reasonable request.

Declarations

Ethics approval All procedures performed in studies involving human participants were in accordance with the ethical standards of IRB of Asan Medical Center (approval code: 2018-1008) and with the 1964 Helsinki declaration and its later amendments or comparable ethical standards.

Consent to participate Informed consent was waived because of the study's retrospective design.

Consent for publication The authors agree to transfer the publication rights to the journal.

Conflict of interest The authors declare no competing interests.

References

1. Anderson DR, Patella VM (1999) Automated static perimetry, 2nd edn. Mosby, St Louis
2. Sommer A, Katz J, Quigley HA, Miller NR, Robin AL, Richter RC, Witt KA (1991) Clinically detectable nerve fiber atrophy precedes

- the onset of glaucomatous field loss. *Arch Ophthalmol* 109:77–83. <https://doi.org/10.1001/archophth.1991.01080010079037>
3. Sehi M, Zhang X, Greenfield DS, Chung Y, Wollstein G, Francis BA, Schuman JS, Varma R, Huang D, Advanced Imaging for Glaucoma Study Group (2013) Retinal nerve fiber layer atrophy is associated with visual field loss over time in glaucoma suspect and glaucomatous eyes. *Am J Ophthalmol* 155:73–82.e1. <https://doi.org/10.1016/j.ajo.2012.07.005>
 4. Quigley HA, Enger C, Katz J, Sommer A, Scott R, Gilbert D (1994) Risk factors for the development of glaucomatous visual field loss in ocular hypertension. *Arch Ophthalmol* 112:644–649. <https://doi.org/10.1001/archophth.1994.01090170088028>
 5. Kuang TM, Zhang C, Zangwill LM, Weinreb RN, Medeiros FA (2015) Estimating lead time gained by optical coherence tomography in detecting glaucoma before development of visual field defects. *Ophthalmology* 122:2002–2009. <https://doi.org/10.1016/j.ophtha.2015.06.015>
 6. Zhang X, Loewen N, Tan O, Greenfield DS, Schuman JS, Varma R, Huang D, Advanced Imaging for Glaucoma Study Group (2016) Predicting development of glaucomatous visual field conversion using baseline Fourier-domain optical coherence tomography. *Am J Ophthalmol* 163:29–37. <https://doi.org/10.1016/j.ajo.2015.11.029>
 7. Jia Y, Wei E, Wang X, Zhang X, Morrison JC, Parikh M, Lombardi LH, Gattley DM, Armour RL, Edmunds B, Kraus MF, Fujimoto JG, Huang D (2014) Optical coherence tomography angiography of optic disc perfusion in glaucoma. *Ophthalmology* 121:1322–1332. <https://doi.org/10.1016/j.ophtha.2014.01.021>
 8. Chung JK, Hwang YH, Wi JM, Kim M, Jung JJ (2017) Glaucoma diagnostic ability of the optical coherence tomography angiography vessel density parameters. *Curr Eye Res* 42:1458–1467. <https://doi.org/10.1080/02713683.2017.1337157>
 9. Moghimi S, Zangwill LM, Penteado RC, Hasenstab K, Ghahari E, Hou H, Christopher M, Yarmohammadi A, Manalastas PIC, Shoji T, Bowd C, Weinreb RN (2018) Macular and optic nerve head vessel density and progressive retinal nerve fiber layer loss in glaucoma. *Ophthalmology* 125:1720–1728. <https://doi.org/10.1016/j.ophtha.2018.05.006>
 10. Shin JW, Song MK, Kook MS (2021) Association between progressive retinal capillary density loss and visual field progression in open-angle glaucoma patients according to disease stage. *Am J Ophthalmol* 226:137–147. <https://doi.org/10.1016/j.ajo.2021.01.015>
 11. Nishida T, Moghimi S, Wu JH, Chang AC, Diniz-Filho A, Kamalipour A, Zangwill LM, Weinreb RN (2022) Association of initial optical coherence tomography angiography vessel density loss with faster visual field loss in glaucoma. *JAMA Ophthalmol* 140:319–326. <https://doi.org/10.1001/jamaophthl.2021.6433>
 12. Yarmohammadi A, Zangwill LM, Diniz-Filho A, Saunders LJ, Suh MH, Wu Z, Manalastas PIC, Akagi T, Medeiros FA, Weinreb RN (2017) Peripapillary and macular vessel density in patients with glaucoma and single-hemifield visual field defect. *Ophthalmology* 124:709–719. <https://doi.org/10.1016/j.ophtha.2017.01.004>
 13. Akagi T, Iida Y, Nakanishi H, Terada N, Morooka S, Yamada H, Hasegawa T, Yokota S, Yoshikawa M, Yoshimura N (2016) Microvascular density in glaucomatous eyes with hemifield visual field defects: an optical coherence tomography angiography study. *Am J Ophthalmol* 168:237–249. <https://doi.org/10.1016/j.ajo.2016.06.009>
 14. Pradhan ZS, Dixit S, Sreenivasaiah S, Rao HL, Venugopal JP, Devi S, Webers CAB (2018) A sectoral analysis of vessel density measurements in perimetrically intact regions of glaucomatous eyes: an optical coherence tomography angiography study. *J Glaucoma* 27:525–531. <https://doi.org/10.1097/IJG.0000000000000950>
 15. Anderson DR, Patella VM (1992) Automated static perimetry. Mosby, St Louis
 16. Budenz DL (1997) Atlas of visual fields. Lippincott-Raven, Philadelphia
 17. Suh MH, Zangwill LM, Manalastas PI, Belghith A, Yarmohammadi A, Medeiros FA, Diniz-Filho A, Saunders LJ, Weinreb RN (2016) Deep retinal layer microvasculature dropout detected by the optical coherence tomography angiography in glaucoma. *Ophthalmology* 123:2509–2518. <https://doi.org/10.1016/j.ophtha.2016.09.002>
 18. Lee JY, Shin JW, Song MK, Hong JW, Kook MS (2021) An increased choroidal microvasculature dropout size is associated with progressive visual field loss in open-angle glaucoma. *Am J Ophthalmol* 223:205–219. <https://doi.org/10.1016/j.ajo.2020.10.018>
 19. Jo YH, Kwon J, Shon K, Jeong D, Kook MS (2019) Greater severity of glaucomatous damage in eyes with than without choroidal microvasculature dropout in open-angle glaucoma. *Invest Ophthalmol Vis Sci* 60:901–912. <https://doi.org/10.1167/iovs.18-26298>
 20. Kwon J, Shin JW, Lee J, Kook MS (2018) Choroidal microvasculature dropout is associated with parafoveal visual field defects in glaucoma. *Am J Ophthalmol* 188:141–154. <https://doi.org/10.1016/j.ajo.2018.01.035>
 21. Kwon JM, Weinreb RN, Zangwill LM, Suh MH (2019) Parapapillary deep-layer microvasculature dropout and visual field progression in glaucoma. *Am J Ophthalmol* 200:65–75. <https://doi.org/10.1016/j.ajo.2018.12.007>
 22. Jonas JB, Martus P, Budde WM, Junemann A, Hayler J (2002) Small neuroretinal rim and large parapapillary atrophy as predictive factors for progression of glaucomatous optic neuropathy. *Ophthalmology* 109:1561–1567. [https://doi.org/10.1016/s0161-6420\(02\)01098-9](https://doi.org/10.1016/s0161-6420(02)01098-9)
 23. Mitchell P, Leung H, Wang JJ, Rochtchina E, Lee AJ, Wong TY, Klein R (2005) Retinal vessel diameter and open-angle glaucoma: the Blue Mountains Eye Study. *Ophthalmology* 112:245–250. <https://doi.org/10.1016/j.ophtha.2004.08.015>
 24. Kass MA, Heuer DK, Higginbotham EJ, Johnson CA, Keltner JL, Miller JP, Parrish RK, 2nd, Wilson MR, Gordon MO (2002) The Ocular Hypertension Treatment Study: a randomized trial determines that topical ocular hypotensive medication delays or prevents the onset of primary open-angle glaucoma. *Arch Ophthalmol* 120:701–13; discussion 829–30. <https://doi.org/10.1001/archophth.120.6.701>
 25. Lalezary M, Medeiros FA, Weinreb RN, Bowd C, Sample PA, Tavares IM, Tafreshi A, Zangwill LM (2006) Baseline optical coherence tomography predicts the development of glaucomatous change in glaucoma suspects. *Am J Ophthalmol* 142:576–582. <https://doi.org/10.1016/j.ajo.2006.05.004>
 26. Anraku A, Enomoto N, Takeyama A, Ito H, Tomita G (2014) Baseline thickness of macular ganglion cell complex predicts progression of visual field loss. *Graefes Arch Clin Exp Ophthalmol* 252:109–115. <https://doi.org/10.1007/s00417-013-2527-9>
 27. Zhang X, Dastiridou A, Francis BA, Tan O, Varma R, Greenfield DS, Schuman JS, Sehi M, Chopra V, Huang D, Advanced Imaging for Glaucoma Study Group (2016) Baseline Fourier-domain optical coherence tomography structural risk factors for visual field progression in the Advanced Imaging for Glaucoma Study. *Am J Ophthalmol* 172:94–103. <https://doi.org/10.1016/j.ajo.2016.09.015>
 28. Sung KR, Kim S, Lee Y, Yun SC, Na JH (2011) Retinal nerve fiber layer normative classification by optical coherence tomography for prediction of future visual field loss. *Invest Ophthalmol Vis Sci* 52:2634–2639. <https://doi.org/10.1167/iovs.10-6246>
 29. Moghimi S, Bowd C, Zangwill LM, Penteado RC, Hasenstab K, Hou H, Ghahari E, Manalastas PIC, Proudfoot J, Weinreb RN (2019) Measurement floors and dynamic ranges of OCT and OCT angiography in glaucoma. *Ophthalmology* 126:980–988. <https://doi.org/10.1016/j.ophtha.2019.03.003>
 30. Mwanza JC, Kim HY, Budenz DL, Warren JL, Margolis M, Lawrence SD, Jani PD, Thompson GS, Lee RK (2015) Residual and dynamic

- range of retinal nerve fiber layer thickness in glaucoma: comparison of three OCT platforms. *Invest Ophthalmol Vis Sci* 56:6344–6351. <https://doi.org/10.1167/iovs.15-17248>
31. Mwanza JC, Budenz DL, Warren JL, Webel AD, Reynolds CE, Barbosa DT, Lin S (2015) Retinal nerve fibre layer thickness floor and corresponding functional loss in glaucoma. *Br J Ophthalmol* 99:732–737. <https://doi.org/10.1136/bjophthalmol-2014-305745>
 32. Miraftebi A, Amini N, Morales E, Henry S, Yu F, Afifi A, Coleman AL, Caprioli J, Nouri-Mahdavi K (2016) Macular SD-OCT outcome measures: comparison of local structure-function relationships and dynamic range. *Invest Ophthalmol Vis Sci* 57:4815–4823. <https://doi.org/10.1167/iovs.16-19648>
 33. Hood DC, Anderson SC, Wall M, Kardon RH (2007) Structure versus function in glaucoma: an application of a linear model. *Invest Ophthalmol Vis Sci* 48:3662–3668. <https://doi.org/10.1167/iovs.06-1401>
 34. Ishikawa H, Stein DM, Wollstein G, Beaton S, Fujimoto JG, Schuman JS (2005) Macular segmentation with optical coherence tomography. *Invest Ophthalmol Vis Sci* 46:2012–2017. <https://doi.org/10.1167/iovs.04-0335>
 35. Tan O, Li G, Lu AT, Varma R, Huang D, Advanced Imaging for Glaucoma Study Group (2008) Mapping of macular substructures with optical coherence tomography for glaucoma diagnosis. *Ophthalmology* 115:949–956. <https://doi.org/10.1016/j.ophtha.2007.08.011>
 36. Kim YK, Ha A, Na KI, Kim HJ, Jeoung JW, Park KH (2017) Temporal relation between macular ganglion cell–inner plexiform layer loss and peripapillary retinal nerve fiber layer loss in glaucoma. *Ophthalmology* 124:1056–1064. <https://doi.org/10.1016/j.ophtha.2017.03.014>
 37. Kim EK, Park HL, Hong KE, Shin DY, Park CK (2021) Investigation of progression pattern and associated risk factors in glaucoma patients with initial paracentral scotomas using Humphrey 10–2. *Sci Rep* 11:18609. <https://doi.org/10.1038/s41598-021-97446-6>
 38. Shin JW, Lee J, Kwon J, Jo Y, Jeong D, Shon G, Kook MS (2019) Relationship between macular vessel density and central visual field sensitivity at different glaucoma stages. *Br J Ophthalmol* 103:1827–1833. <https://doi.org/10.1136/bjophthalmol-2018-313019>
 39. Mikelberg FS, Drance SM (1985) The mode of progression of visual field defects in glaucoma. In: Heijl A, Grave EL (eds) Sixth International Visual Field Symposium. Springer, Dordrecht, pp 387–390
 40. Mikelberg FS, Schulzer M, Drance SM, Lau W (1986) The rate of progression of scotomas in glaucoma. *Am J Ophthalmol* 101:1–6. [https://doi.org/10.1016/0002-9394\(86\)90457-5](https://doi.org/10.1016/0002-9394(86)90457-5)
 41. Boden C, Blumenthal EZ, Pascual J, McEwan G, Weinreb RN, Medeiros F, Sample PA (2004) Patterns of glaucomatous visual field progression identified by three progression criteria. *Am J Ophthalmol* 138:1029–1036. <https://doi.org/10.1016/j.ajo.2004.07.003>
 42. De Moraes CG, Juthani VJ, Liebmann JM, Teng CC, Tello C, Susanna R Jr, Ritch R (2011) Risk factors for visual field progression in treated glaucoma. *Arch Ophthalmol* 129:562–568. <https://doi.org/10.1001/archophthalmol.2011.72>
 43. Hou H, Moghimi S, Proudfoot JA, Ghahari E, Pentead RC, Bowd C, Yang D, Weinreb RN (2020) Ganglion cell complex thickness and macular vessel density loss in primary open-angle glaucoma. *Ophthalmology* 127:1043–1052. <https://doi.org/10.1016/j.ophtha.2019.12.030>
 44. Shin JW, Sung KR, Song MK (2020) Ganglion cell-inner plexiform layer and retinal nerve fiber layer changes in glaucoma suspects enable prediction of glaucoma development. *Am J Ophthalmol* 210:26–34. <https://doi.org/10.1016/j.ajo.2019.11.002>
 45. Yu M, Lin C, Weinreb RN, Lai G, Chiu V, Leung CK (2016) Risk of visual field progression in glaucoma patients with progressive retinal nerve fiber layer thinning: a 5-year prospective study. *Ophthalmology* 123:1201–1210. <https://doi.org/10.1016/j.ophtha.2016.02.017>
 46. Shin JW, Sung KR, Lee GC, Durbin MK, Cheng D (2017) Ganglion cell-inner plexiform layer change detected by optical coherence tomography indicates progression in advanced glaucoma. *Ophthalmology* 124:1466–1474. <https://doi.org/10.1016/j.ophtha.2017.04.023>
 47. Hood DC, Raza AS, de Moraes CG, Liebmann JM, Ritch R (2013) Glaucomatous damage of the macula. *Prog Retin Eye Res* 32:1–21. <https://doi.org/10.1016/j.preteyeres.2012.08.003>
 48. Traynis I, De Moraes CG, Raza AS, Liebmann JM, Ritch R, Hood DC (2014) Prevalence and nature of early glaucomatous defects in the central 10 degrees of the visual field. *JAMA Ophthalmol* 132:291–297. <https://doi.org/10.1001/jamaophthalmol.2013.7656>
 49. Martinez A, Gonzalez F, Capeans C, Perez R, Sanchez-Salorio M (1999) Dorzolamide effect on ocular blood flow. *Invest Ophthalmol Vis Sci* 40:1270–1275
 50. He L, Ren R, Yang H, Hardin C, Reyes L, Reynaud J, Gardiner SK, Fortune B, Demirel S, Burgoyne CF (2014) Anatomic vs. acquired image frame discordance in spectral domain optical coherence tomography minimum rim measurements. *PLoS One* 9:e92225. <https://doi.org/10.1371/journal.pone.0092225>

Publisher's Note Springer Nature remains neutral with regard to jurisdictional claims in published maps and institutional affiliations.

Springer Nature or its licensor (e.g. a society or other partner) holds exclusive rights to this article under a publishing agreement with the author(s) or other rightsholder(s); author self-archiving of the accepted manuscript version of this article is solely governed by the terms of such publishing agreement and applicable law.